The Astronomical Journal, 154:36 (7pp), 2017 July https://doi.org/10.3847/1538-3881/aa77fe

Measuring the Meteoroid Environments of the Planets with Meteor Detectors on Earth

Paul Wiegert[1,2], Peter Brown[1,2], Petr Pokorny[3], Karina Lenartowicz[1], and Zbyszek Krzeminski[1]
[1] Dept. of Physics and Astronomy, The University of Western Ontario London, Canada; pwiegert@uwo.ca
[2] Centre for Planetary Science and Exploration (CPSX), The University of Western Ontario London, Canada
[3] Dept. of Physics, The Catholic University of America, Washington D.C., USA
Received 2017 April 3; revised 2017 May 16; accepted 2017 May 28; published 2017 July 5

Abstract

We describe how meteors recorded at the Earth can be used to partly reconstruct the meteoroid environments of the planets if a large sample (i.e., millions of orbits at a minimum) is available. The process involves selecting from the Earth-based sample those meteors that passed near a planet's orbit prior to arriving at Earth, and so carry information about the planetary meteoroid environment. Indeed, this process can be extended to any location in the solar system, though some regions of space are better sampled than others. From such a reconstruction performed with data from the Canadian Meteor Orbit Radar, we reveal that Mars has apex, helion, anti-helion, and toroidal sporadic sources, much as Earth does. Such reconstructions, albeit partial, have the potential to provide a wealth of detail about planetary meteoroid environments and to allow for the ground-truthing of model meteoroid populations without in situ sampling.

Key words: comets: general – meteorites, meteors, meteoroids – planets and satellites: general

1. Introduction

The meteoroid environment at the Earth has been measured over a large particle size range by a number of techniques, while the environments of the other planets are much less well known. The difference is largely due to the fact that the equipment used to measure meteors at the Earth, such as camera networks and meteor radars, which use the atmosphere as a detector, cannot easily be transported and deployed on other planets by spacecraft.

Some dust measurements have been performed of the meteoroid environment away from Earth, (Staubach et al. 2002). However, these are primarily in situ measurements by spacecraft impact detectors and therefore limited to small collecting areas. As recent examples, the Cosmic Dust Detector on the *Cassini* spacecraft at Saturn (Kempf et al. 2004; Srama et al. 2004), and the Student Dust Counter on the New Horizons mission to Pluto (Horányi et al. 2008; Poppe et al. 2010; Szalay et al. 2013) both have sensitive areas of only 0.1 m^2. They are therefore unable to sample particles much larger than a few microns. In contrast, ground-based meteor detectors might monitor thousands of square km of sky or more e.g., $\sim 10^6$ km^2 for the European Fireball Network (Oberst et al. 1998).

Several works have predicted the existence of meteor showers on other planets based on known comet/meteoroid stream orbits (e.g., Selsis et al. 2004; Christou 2010) with close nodal points to other planetary orbits. However, observations of planetary meteoroid environments (PMEs) other than Earth at sizes larger than a few microns are limited to a short optical survey at Mars (Domokos et al. 2007), individual impacts in the Jovian atmosphere (Hueso et al. 2013), and indirect inference of meteoroid impacts on Mercury based on exospheric gas measurements (Christou et al. 2015).

Here, we report on a technique that allows us to study the meteoroid environment at a planet in our solar system, directly measured from Earth. This works for any solar system planet and indeed arbitrary locations in interplanetary space. It uses the same equipment as Earth-based meteor studies, whether camera, radar, or otherwise. It simply involves selecting from the observed terrestrial meteoroid orbit sample those particles that passed near the orbit of another planet prior to arriving at Earth. Particles that pass near a planet before arriving at Earth are *de facto* part of that planet's meteoroid environment, and recognizing them as such, we can partially reconstruct the PME through inversion of these carefully chosen meteoroid orbits as observed at Earth. An important obstacle for this technique is the small number of meteoroids travelling from the vicinity of any given planet to Earth. As a result, a necessary condition for this technique to be useful is a large sample of measured meteoroid orbits. We can improve our sampling if we are willing to assume that the meteoroid environment of the planets is approximately azimuthally symmetric about its orbit: this is known to be approximately true for the Earth (Campbell-Brown & Jones 2006). In this case, the sample of meteoroids measured at Earth that pass sufficiently near the *orbit* of a given planet (rather than those that pass sufficiently near the planet itself) provides a proxy for the time-averaged PME. Given sufficient numbers of meteoroid orbits, we will show that such a sub-sampling provides useful information on PMEs and show that from it, we can predict (as just one example) that features in the spatial radiant distribution at Mars are reminiscent of those seen in the sporadic distribution at Earth.

This approach is not without its limitations: geometrical restrictions arise from the need for the meteoroid orbit to pass near both the planet in question and the Earth. We also need a *very* large sample of meteors to get usable statistics. Here, the Canadian Meteor Orbit Radar (CMOR, Webster et al. 2004), which measured over 4.3 million meteors orbits in the interval 2011–2014, is the sample that will be used. Even with this vast data set, only a small fraction ($\sim$1%) are usable for our purposes: a smaller data set will scarcely do. Nonetheless, partial data is better than none, and it provides a first look at what otherwise would remain undetected entirely.

2. Method

Our intent here is to provide a proof of concept and present an initial reconnaissance of what portions of the PMEs can be sampled from Earth and what they look like in their broad

strokes. The key to this technique is determining which of the CMOR meteoroid orbits passed near the orbit of another planet prior to its detection at Earth. The CMOR meteor patrol radar has been described elsewhere (Webster et al. 2004). Here, we will use the data measured from CMOR since 2011, as this is the time period after which a total of six stations began operation (Brown et al. 2012) from an original network of three, and, hence, the precision of orbits is significantly better on the average since 2011. To determine whether a given meteoroid orbit is part of another planet's PME, we compute the Minimum Orbital Intersection Distance (MOID) between its pre-atmospheric orbit and the planet's osculating orbit. If the MOID is less than a particular value (which varies by planet), we will consider it part of our PME sample. The values chosen here are of the same order as the planetary Hill spheres: 0.01 au for the terrestrial planets and 1 au for the outer planets. For this initial study, we will ignore the effects of instrumental error on the MOID calculation, though inclusion of uncertainties could be used to refine the calculated PME.

The sample of CMOR meteoroids that passed near a planet's orbit prior to its arrival at Earth gives us a first look at the PME. To obtain a more quantitative result, we have to consider the efficiency with which particles can travel from the planets to us. There are at least two parts to this calculation.

The first relates to the fraction of meteoroid orbits that have a geometry suitable to reach the Earth; the second has to do with the "field of view" of the radar itself, which cannot observe all radiants that reach our planet. These biases will be addressed in the next two subsections.

2.1. Meteoroid Orbital Transfer Efficiency from the Planets to Earth

Some meteoroids passing near the planet's orbit can reach the Earth, others cannot on purely geometrical grounds. To examine this, we analyze a random sample of hypothetical meteoroids passing near each of the planets to determine which can reach the Earth afterwards. This work is a simple extension of the scattering work done as part of Wiegert (2014) and allows for an assessment of how much of a PME we can hope to sample under ideal conditions.

We will use the planet Mars as an example for concreteness. If we imagine all possible radiant directions and speeds on Mars' meteor sky, some would (if they weren't destroyed by their encounter with Mars) go on to reach Earth. We can numerically compute which of these radiants could have been sampled at Earth, in order to get a picture of the portion of Mars' meteor sky we can, in principle, sample. We refer to the function defining whether or not a given radiant at Mars can reach Earth as the Transfer Function (TF).

To compute the TF, one million hypothetical meteoroids at Mars are created with radiants that are drawn randomly on Mars' sky, and for each, a speed is randomly drawn from a uniform distribution between zero and the heliocentric escape speed at Mars. The fraction of these that could reach Earth are counted. The criterion for reaching Earth is that the meteoroid orbit have a node between 0.9 and 1.1 au from the Sun or that its heliocentric inclination be less than 3° or more than 177°. The inclination choice used is based on the size of the Earth's Hill sphere, 0.01 au, which subtends an angle of 3° when seen from the Sun. The addition of the inclination criterion is a first-order attempt to account for the fact that meteors with orbits very nearly in the plane of Earth's orbit can strike our planet, even if they do not have a node near 1 au; a more sophisticated criterion based on the MOID could be used but is unlikely to affect the results significantly. A plot of the TF for Mars, that is, the meteor radiants at Mars that can reach Earth, is in the top panel of Figure 1.

Each pixel in the top panel of Figure 1 represents the fraction of meteors that arrive at Mars from a particular radiant, and that subsequently can reach Earth. Note that the radiants in Figure 1 are not the meteor's radiants at Earth (which are different), but are those they would have had at the planet itself had they struck it.

Any regions in white in Figure 1 represent "forbidden regions" in that no meteors at any speed considered here can travel from the planet to Earth, and so we are inherently blind to these radiant zones. The meteoroids at Mars that have Martian radiants in the ecliptic plane are the best sampled at Earth; however, there are numerous radiants at higher ecliptic latitudes that are also accessible. If Mars has six sporadic meteor sources similar to those at Earth (Jones & Brown 1993), the top panel of Figure 1 indicates that we can expect to sample all of them from Earth, though many only at a very low level (∼5%). Nonetheless, this provides a first important result from this work: meteor detectors on Earth have access to a fraction of the meteoroid environment at Mars and, in fact, at the other planets as well, as will be described later.

Our transfer efficiency is idealized for simplicity. It assumes that both the Earth and Mars are on circular orbits, that the meteoroid was not appreciably deflected by the planet when it passed it, and that the intersection criterion described above is applicable. Though reasonable approximations, they are not perfect, and as a result, we will occasionally find that CMOR meteors are detected from these forbidden regions. However, these discrepancies do not affect our broader argument.

The TFs for other planets are also shown in the lower panels of Figure 1. The fraction of meteors that can reach Earth from each of the planet's PME is shown in Table 1 and ranges from 9.0% at Mars down to 2.8% for Mercury. Thus, a wide range of radiants across a planet's meteor sky are, in principle, accessible from Earth. As a rule, the ecliptic plane is always best sampled, as the geometrical intersection constraint is easier to satisfy. The apex region (near the zero of the apex-centered ecliptic latitude and longitude) is often completely inaccessible, but much of the rest of the planet's meteor sky is sampled at some level.

The idealized TF described above allows us to assess how much of the available phase space can be measured from Earth. Also interesting is the fraction of the *populated* phase space at each planet that can reach Earth. This is, of course, unknown at this time, but we can use a model of each planet's meteoroid environment as a proxy. Here, we use the PME model of Wiegert et al. (2009), a physics-based self-consistent model of the near-Earth meteoroid environment calibrated to CMOR data. Though constructed specifically for Earth, the model contains information on the PMEs of all the planets. The terrestrial planets will be reasonably well-represented by this model, but it was not designed for the outer planets. The fraction of each model PME that can be sampled at Earth is in line 2 of Table 1. Here, we see that the Wiegert et al. (2009) model predictions suggest an even larger fraction of the terrestrial PMEs are accessible to us than was suggested by our uniform model : 9% for Mercury, 14% for Mars, and 24% for Venus. The fraction is reduced for the outer planets, to between 1% and 3% in all cases.

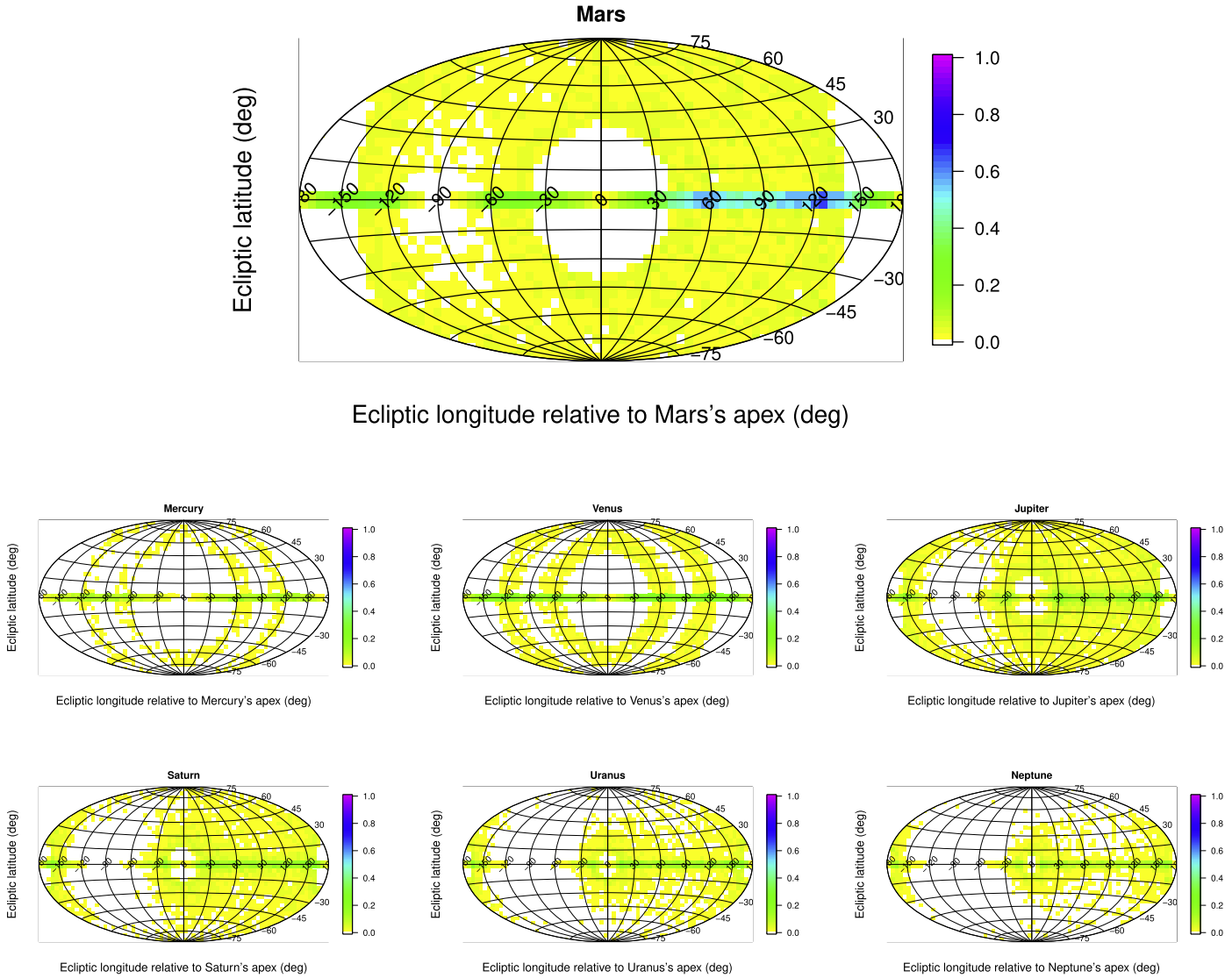

Figure 1. The meteor sky at each planet color-coded by the fraction of radiants that can reach the Earth, in apex-centered coordinates. The apex of the planet's way is in the center; the Sun is at -90° longitude and opposition at $+90^\circ$. White regions indicate radiants for which less than 0.1% of the possible speeds can reach Earth.

We conclude that planetary PMEs can be measured at a significant level from Earth, given a sufficiently large sample of meteoroid orbits. In particular, these measurements offer the possibility of "ground-truthing" and calibrating dynamical models of PMEs without in situ measurements.

2.2. *The Observational Geometry from the CMOR Radar*

Having assessed, in the previous section, that a reconstruction of PMEs is possible in principle, we turn to the observing biases that affect this process. Located in the northern hemisphere, CMOR ($43^\circ16'$ N, $80^\circ46'$ W) can only see meteors arriving from certain directions. CMOR has a nearly all-sky gain pattern, which means that most radiants that get above the local horizon have some detectability throughout the day. Due to this broad beam pattern, the time-weighted radiant collecting area is purely a function of declination, as discussed in Campbell-Brown & Jones (2006). To determine the effect of this on our sample, we calculate the relative collecting area f of the radar as a function of the radiant declination of the arriving meteor. Here, we take f to be the time average over the year of the cosine of the angle between a given apparent meteor radiant and the local vertical at the radar site, with any negative values (radiant below the horizon) taken to be zero. Thus, a radiant that was never above CMOR's horizon would have $f = 0$. In practice, a radiant at the North equatorial Pole has the highest effective value at $\sin(43^\circ16') = 0.69$, a result also found in Campbell-Brown & Jones (2006; see their Figure 6).

A weighting of $1/f$ is then applied to that meteor to allow for the radar's time-integrated collecting area for that radiant. Radiants with $f = 0$ are not weighted; they cannot be measured with CMOR but are designated "inaccessible" (see next section).

There are other observing biases that generically affect backscatter radar measurements of meteors (Galligan & Baggaley 2004). For CMOR, the most important is the echo height ceiling (which reduces sensitivity to higher-speed meteoroids, e.g., Campbell-Brown & Jones 2003) and the ionization efficiency, which reduces detectability of slower meteoroids (Ye et al. 2016), favoring detection of larger, slower meteoroids. Although these are important for the construction of the best possible PME, we ignore these effects for simplicity, as our efforts here are toward a proof of concept rather than a high-precision result. Moreover, these effects tend to be size-dependent, and as we do

Table 1
Percent of Meteor Radiants at a Planet that Reach Earth

Name	Mercury	Venus	Mars	Jupiter	Saturn	Uranus	Neptune
Uniform (%)	2.8	5.2	9.0	6.2	5.5	4.3	3.5
WCBV09 (%)	8.7	23.7	14.4	2.0	1.3	1.3	2.6

Note. Uniform refers to a random-on-the-sphere distribution of radiants at all speeds from zero to the local heliocentric escape speed. WCBV09 uses the radiant and speed distribution from the planetary meteoroid model of Wiegert et al. (2009).

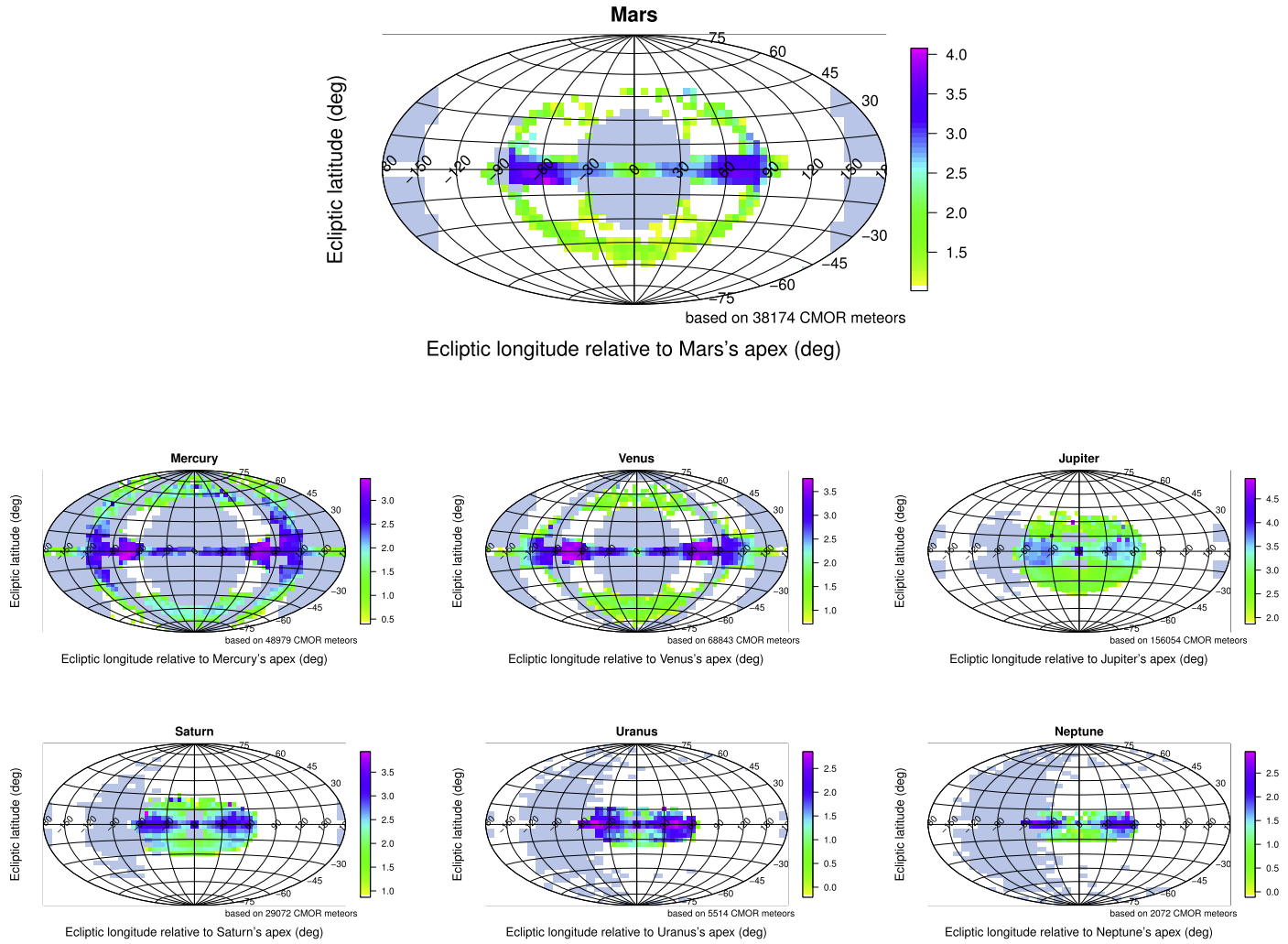

Figure 2. Radiant distribution of CMOR-detected meteors at Earth that pass within 0.01 au of the terrestrial planets' orbits (1 au for outer planets), in apex-centered ecliptic coordinates at the planet. The scale is the base-10 logarithm of the weighted number of meteors at each radiant. The apex of the planet's way is in the center; the Sun is at −90° longitude and opposition at +90°. Pixels in gray indicate forbidden regions from which less than 1% of possible speeds from those radiants can reach the Earth (i.e., the TF is less than 0.01); white pixels indicate radiants for which at least some meteors could reach the Earth (i.e., the TF is greater than 0.01) but none are observed by CMOR.

not use size-frequency distribution in any of our models, as long as CMOR can detect some fraction of the population from any radiant, we can use it to probe other PMEs. We also note that we adopt a simple frequentist approach to debiasing the sample here, but Bayesian techniques are likely to perform better when a more complete reconstruction of PMEs is attempted.

3. Results

3.1. Meteoroid Environments at the Planets

In order to reconstruct the PMEs, each CMOR meteoroid deemed to have arrived from a PME is assigned a weight that is inversely proportional to the relative collecting area of the radar. No correction for the TF is applied because the correct TF to apply depends on the PME in question, which is a priori unknown. We do note that the sporadic meteor sources are known to have very broad-speed distributions at the Earth (Jones & Brown 1993), and so a correction based on the uniform TF might be correct to zeroth order. A more accurate approach could involve comparison with a model distribution and/or "best-fit" approach but this is beyond the scope of this paper; our intent here is simply to provide a first look at what can be recovered about PMEs from Earth-based samples.

To present our results, we again use Mars as our prototype. The reconstructed radiant distribution at this planet is shown in the top panel of Figure 2, from 38178 CMOR meteors collected from 2011 to 2014 (about 1% of the total) whose orbits, when traced backward, have MOIDs with 0.01 au of Mars' orbit.

The most prominent features are the Martian helion and anti-helion sporadic sources, the regions at zero latitude near -90° and $+90^\circ$ in apex-centered longitude, respectively. The north and south toroidal sporadic sources, at $\pm 60^\circ$ latitude and zero longitude on Earth are well-measured. In fact, the south toroidal source is quite distinct in the figure. The north toroidal source, which is comparable in strength to the southern on Earth, is absent. However, this is likely a selection effect due to the geometrical constraint of having a node both at Mars and the Earth. CMOR is in Earth's northern hemisphere and detects meteoroids that are mostly at their descending node at Earth. These same particles are at their ascending node at Mars, and, hence, strike it from the south. Given the near mirror symmetry around the ecliptic plane of the Earth's PME, it is likely that Mars does in fact have north and south toroidal sources of comparable strength. The northern toroidal source cannot be said to be weaker based solely on these measurements; rather, we would contend that CMOR's sensitivity to the Mars northern toroidal source is much less. Clearly it would be advantageous to combine meteor data sets obtained from Earth's northern and southern hemispheres (e.g., Pokorný et al. 2017) to provide a better picture.

The apex sources near zero longitude and latitude are mostly inaccessible, in a region where the TF is zero, but are sampled much better along the ecliptic. The apex sources on Earth are associated with retrograde meteors and, hence, with the highest speeds relative to the planet. The top panel of Figure 3 shows the speed distribution at Mars. At the Earth, the overall speed distribution has two peaks, one at $30\,\mathrm{km\,s^{-1}}$ and one at $55\,\mathrm{km\,s^{-1}}$ (Taylor 1995; Sato et al. 2000; Close et al. 2002; Janches et al. 2003; Chau & Woodman 2004; Galligan & Baggaley 2004; Hunt et al. 2004; Chau et al. 2007; Janches et al. 2008; Wiegert et al. 2009). The higher-speed peak is associated with the apex sources. The fact that the distribution at Mars shows two similar peaks indicates that our technique encompasses a broad subset of the PME. In particular, the presence of the small higher-speed peak in the top panel of Figure 3 near $50\,\mathrm{km\,s^{-1}}$ at Mars confirms that we can sample a subset of the high-speed Martian apex sporadic meteoroid population at Earth.

From these results, we predict with some confidence that Mars has helion, anti-helion, and south toroidal sporadic sources, and probably a north toroidal source. The apex sources are not evident in the radiant map, but the speed distribution suggests that they are being sampled, albeit much more thinly, likely due to the low TF.

The meteoroid environment for the other planets, indeed for any location within the solar system, can be reconstructed in the same manner. Here, we present the results for the radiant distributions at the other planets in Figure 2 and the speed distributions in Figure 3. These are reconstructed from samples with sizes ranging from the lowest at 2072 meteors for Neptune to the largest at 156,054 meteors for Jupiter, or 0.05%–3.6% respectively of the 4.3 million meteors collected by CMOR from 2011 to 2014. We emphasize that this represents only part of the PME at each planet. However, the fact that there are radiants that are accessible through high TF at Earth from a given planet but not represented in CMOR measurements, is an important constraint not previously known for different PMEs.

For the other terrestrial planets, the sporadic radiant features seen resemble those for Mars. There are prominent helion and anti-helion sporadic sources near $\pm 90^\circ$ from the apex, with a strong band stretching through the apex sources. The toroidal regions are less distinct but represented. The speed distributions show a clear bi-modality, again very similar to what is observed at Earth.

For the giant planets, we see meteors only in the region around the apex source, and there is a clear concentration of orbits in the ecliptic plane. Though portions of the helion and toroidal sources are notionally observable, we do not see any meteors from these regions for any of the outer planets. However, we recall that the white regions in Figure 2 are those where meteors at some speed from zero to the heliocentric escape speed could reach us, not necessarily those speeds that are actually populated at these planets. Thus, the absence of toroidal or helion sources from these figures is not enough to conclude that there are no such meteors at the planet's themselves. They may exist, but at speeds that result in orbits that do not reach us at Earth. In a similar vein, the density enhancements of radiants shown in Figure 2 are subject to the same biases and could be significantly affected by the absence from our sample of the meteor component that simply cannot reach Earth. This geometrical constraint, that we can only measure orbits passing near both the Earth and our planet, means that the measurement of some components of PMEs will necessarily have to await in situ measurements.

4. Conclusions

Examination of the phase space in the meteoroid environments for each of the planets reveals that a few to several percent of the meteoroids that have orbits passing close to other planetary orbits in the solar system can reach the Earth. From this, we conclude that some measurement of these environments is possible with Earth-based equipment, if we can obtain a sufficiently large sample. Additionally, that calibration and ground-truthing of model meteoroid environments is possible in principle, without the need to measure the planetary environment in situ.

A large sample of CMOR radar meteors observed at the Earth was then examined to find those that are also part of the meteoroid environments of other planets, and a partial meteoroid environment was reconstructed for each of the planets. Although only partial, this reconstruction allows us to predict features similar to the sporadic meteor sources observed at Earth in the environments of Mars and the other terrestrial planets. For the outer planets, high-speed retrograde meteors from their apex sources are the best sampled. From CMOR observations of the meteoroid environment at Earth and our model, we predict a concentration of radiants in the ecliptic, but we have much sparser information on the existence of helion, anti-helion, or toroidal sporadic sources.

Thus, the first measurements of the meteoroid environments of the planets have now been made. In future works, through more careful corrections for the observational biases, larger CMOR data sets, and higher-fidelity modeling, we believe the construction of well-calibrated models of other PMEs is possible.

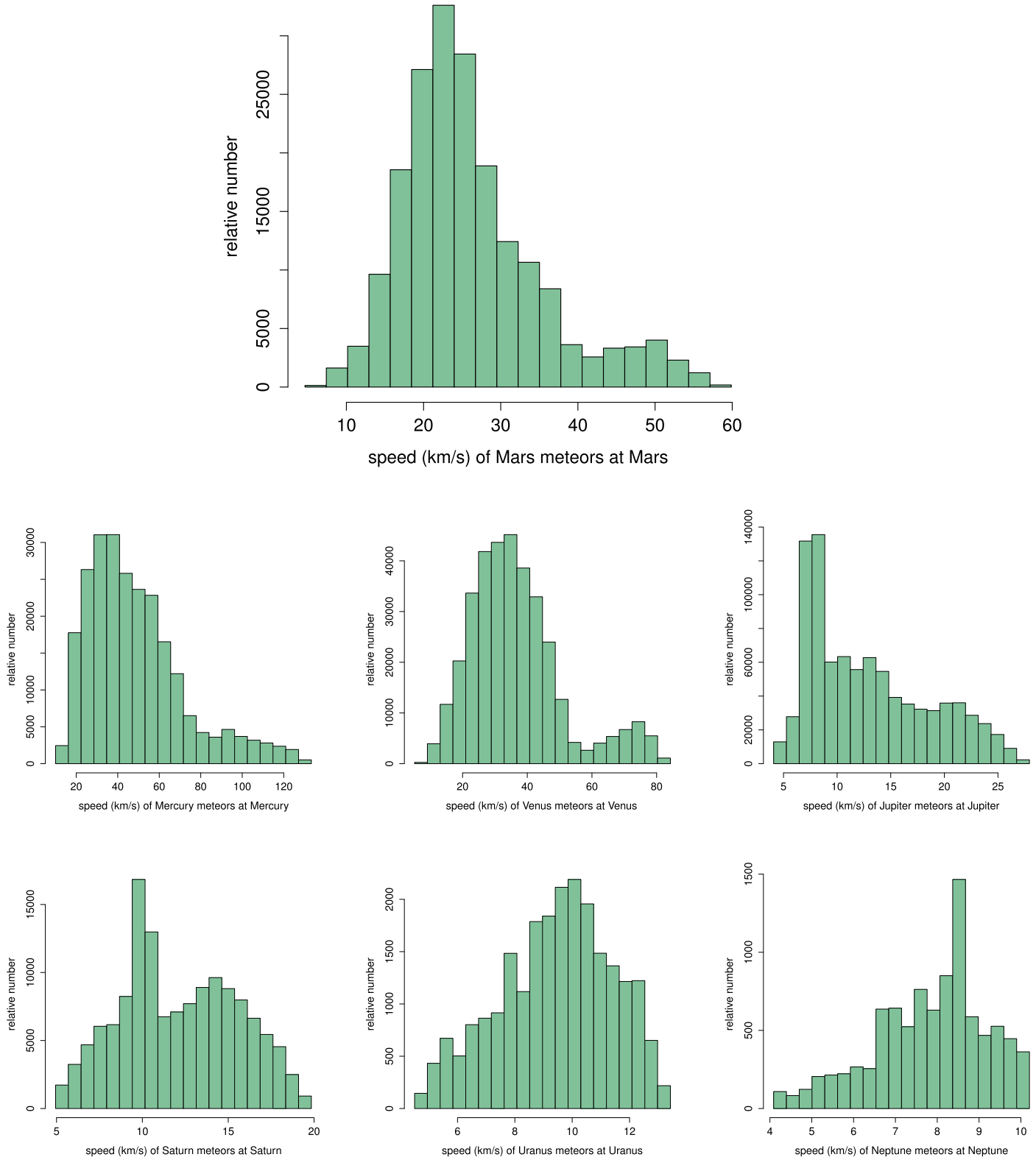

Figure 3. Meteoroid speed distribution, showing the speeds that would be measured at the planet, based on those CMOR meteors detected at Earth that intersect the planet's orbit.

P.G.B. wishes to thank the Canada Research Chair program. This work was supported in part by the Natural Sciences and Engineering Research Council of Canada and NASA's Meteoroid Environment Office (MEO) through co-operative agreement NNX15AC94A.

References

Brown, P. G., Weryk, R. J., Wong, D. K., & Campbell-Brown, M. D. 2012, in American Astronomical Society, DPS Meeting 44, 302.04
Campbell-Brown, M. D., & Jones, J. 2003, MNRAS, 343, 775
Campbell-Brown, M. D., & Jones, J. 2006, MNRAS, 367, 709

Chau, J. L., & Woodman, R. F. 2004, ACP, 4, 511
Chau, J. L., Woodman, R. F., & Galindo, F. 2007, Icar, 188, 162
Christou, A. A. 2010, MNRAS, 402, 2759
Christou, A. A., Killen, R. M., & Burger, M. H. 2015, GeoRL, 42, 7311
Close, S., Oppenheim, M., Hunt, S., & Dyrud, L. 2002, JGRA, 107, 1295
Domokos, A., Bell, J., Brown, P. G., et al. 2007, Icar, 191, 141
Galligan, D. P., & Baggaley, W. 2004, MNRAS, 353, 422
Galligan, D. P., & Baggaley, W. J. 2004, MNRAS, 353, 422
Horányi, M., Hoxie, V., James, D., et al. 2008, SSRv, 140, 387
Hueso, R., Pérez-Hoyos, S., Sánchez-Lavega, A., et al. 2013, A&A, 560, 55
Hunt, S. M., Oppenheim, M., Close, S., et al. 2004, Icar, 168, 34
Janches, D., Close, S., & Fentzke, J. T. 2008, Icar, 193, 105
Janches, D., Nolan, M. C., Meisel, D. D., et al. 2003, JGRA, 108, 1222
Jones, J., & Brown, P. 1993, MNRAS, 265, 524
Kempf, S., Srama, R., Altobelli, N., et al. 2004, Icar, 171, 317
Oberst, J., Molau, S., Heinlein, D., et al. 1998, M&PS, 33, 49
Pokorný, P., Janches, D., Brown, P. G., & Hormaechea, J. L. 2017, Icar, 290, 162
Poppe, A., James, D., Jacobsmeyer, B., & Horányi, M. 2010, GeoRL, 37, L11101
Sato, T., Nakamura, T., & Nishimura, K. 2000, IEICE, E83-B, 1990
Selsis, F., Brillet, J., & Rapaport, M. 2004, A&A, 789, 783
Srama, R., Ahrens, T. J., Altobelli, N., et al. 2004, SSRv, 114, 465
Staubach, P., Grün, E., & Matney, M. 2002, in Interplanetary Dust, ed. E. Grun et al. (Berlin: Springer), 346
Szalay, J. R., Piquette, M., & Horányi, M. 2013, EP&S, 65, 1145
Taylor, A. D. 1995, Icar, 116, 154
Webster, A. R., Brown, P. G., Jones, J., Ellis, K. J., & Campbell-Brown, M. 2004, ACP, 4, 679
Wiegert, P., Vaubaillon, J., & Campbell-Brown, M. 2009, Icar, 201, 295
Wiegert, P. A. 2014, Icar, 242, 112
Ye, Q., Brown, P. G., & Pokorný, P. 2016, MNRAS, 462, 3511